INFLUENCE OF THE BOUNDARY CONDITIONS ON THE DISPLACEMENT CAPACITY OF URM PIERS

S. Petry[1] and K. Beyer[2]

[1] PhD student, Earthquake Engineering and Structural Dynamics Laboratory (EESD), School of Architecture, Civil and Environmental Engineering (ENAC), Ecole Polytechnique Fédérale de Lausanne (EPFL), Lausanne, Switzerland, sarah.petry@epfl.ch

[2] Assistant Professor, Earthquake Engineering and Structural Dynamics Laboratory (EESD), School of Architecture, Civil and Environmental Engineering (ENAC), Ecole Polytechnique Fédérale de Lausanne (EPFL), Lausanne, Switzerland, katrin.beyer@epfl.ch

ABSTRACT

Existing recommendations estimate the drift capacity of unreinforced masonry (URM) piers as a function of the failure mode. The empirical relationships are based on results from quasi-static cyclic tests on single U RM piers, which were test ed simulating either fixed-fixed or cantilever boundary conditions. In real stru ctures, the verti cal URM piers are conn ected to each other by horizontal structural elem ents such as slabs and spandrels that provide a coupling action. Depending on the stiffness and strength of these horizontal elements, the boundary conditions of the piers vary significantly.

In order to investigate the influence of the bounda ry conditions, three quasi-static cyclic tests on identical URM piers were performed. All piers were subjected to the s ame vertical load but the boundary conditions for the lateral loading were varied. For the first pier, fixed-fixed boundary conditions with zero rotation at the top were sim ulated. For the second and third piers, the moment applied at the top of the pier was proportional to the applied horizontal load and therefore the height of zero m oment was constant at 0.75 and 1.5 tim es the pier height for the second and third pier, respectively. This paper pr esents preliminary results of the tests on these piers and discusses the influence of the bounda ry conditions on the displacem ent capacity of URM piers. In addition , force and drift capaciti es are co mpared to values p redicted by th e Eurocode.

KEYWORDS: unreinforced m asonry, quasi-static cyclic testing, disp lacement capacities, coupling influence

INTRODUCTION

In unreinforced m asonry (URM) buildings, the pi ers are connected by horizontal structural elements such as slabs and masonry spandrels. When the piers are subjected to in-p lane loading, these horizontal elements act as coupling elem ents between the piers. T he stiffness and streng th of these coupling elem ents can va ry significantly and the literature distinguishes three levels of coupling: (1) weak coupling, where the horizon tal elements impose only equal displacements on the piers of each story but do not transfer significant shear forces or bending moments, (2) strong coupling, where vertical and horizontal elem ents develop together a fram ing action and where the coupling elements remain largely elastic when the struc ture is subjected to hor izontal loading, (3) intermediate coupling, where the mo ment transferred by the coupling elem ents are

limited but not negligible. When considering a first storey pier, the coupling elements influence the rotational restraint at the top of the pier and therefore, the moment profile over the height of the pier. For outer piers, the coupling elements also cause an axial force variation in the pier. For inner piers in a rather symmetrical structure the axial force variation due to the horizontal loading is small and can be neglected.

The objective of an ongoing research project at EPFL is to study the effect of the boundary conditions imposed by the coupling elements on the deformation capacity of the piers. Within the project, quasi-static cyclic tests on URM piers with different boundary conditions were conducted. To determine characteristic boundary conditions of inner piers, a reference building is analysed. The reference building represents a modern masonry building with reinforced concrete (RC) slabs. In such a structure, the coupling action is largely dependent on the assumed effective width and length of the slab. The paper commences therefore with a brief review on recommended values for the effective width and length of RC slabs when analysing URM structures, before the pushover analysis results are presented and reviewed with respect to the moment profile imposed on an inner pier of the first storey. The results of this analysis serve for defining the boundary conditions of the quasi-static cyclic tests on masonry piers. The main part of this paper presents selected results from three tests on URM piers subjected to the same axial load but different boundary conditions.

COUPLING INTRODUCED THROUGH MODERN RC SLABS
Modern masonry structures in Switzerland feature typically RC slabs. The in-plane rigidity of these slabs is sufficient to enforce equal horizontal displacement onto all piers of one story. For out-of-plane bending, with respect to the plane of the slab, the stiffness and strength of the slabs is limited but not negligible and therefore Priestley et al. [1] suggest including the slabs as one-dimensional RC beam elements in equivalent frame models of URM structures. The beams should be assigned an effective beam width $b_{cb,eff}$ and an effective length $l_{cb,eff}$. The effective length can be estimated as [1]:

$$l_{cb,eff} = l_{cb} + 2h_{cb} \tag{1}$$

where l_{cb} is the free span between two piers and h_{cb} the depth of the slab. Priestley et al. [1] recommend taking the width of the equivalent beam $b_{cb,eff}$ as twice to three times the wall thickness and assume that the beam is fixed at both ends. The shear force V_{max} associated with the formation of plastic hinges at the two beam ends can be computed as:

$$V_{max} = \frac{2M_{pl}}{l_{cb,eff}} \tag{2}$$

where M_{pl} is the plastic moment capacity of the beam. If the moment capacity of the beam is large, the coupling beam might remain elastic when the building is subjected to seismic loading and the maximum coupling moment will be limited by the capacity of the piers. Estimates for the displacement capacities of RC beams can be found in the literature, e.g., in [1].

PUSHOVER ANALYSIS OF A REFERENCE STRUCTURE

In order to evaluate the influence of the effective width of the RC slab on the moment profiles of the URM piers of the first storey, a reference structure with both URM and RC walls and RC slabs was analysed (Figure 1.a). Such mixed RC-URM wall structures are typical for residential buildings in Switzerland and a similar structure will be tested at half scale on the shake table of the TREES Laboratory in Pavia, Italy.
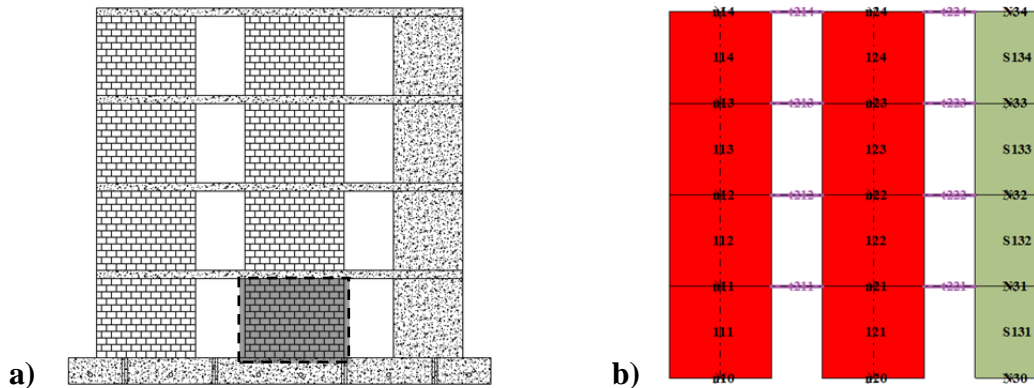

Figure 1: Reference building with URM and RC walls: (a) sketch of the structure with the outlined internal pier at ground floor level, (b) corresponding macro-element model in Tremuri.

The behaviour of the structure was simulated using the software Tremuri, which was developed by Lagomarsino et al. [2] in order to provide a simple tool for engineers to analyse URM structures. All URM piers were modelled with macro-elements [3, 4], which allow considering both shear and rocking failure. The RC piers were simulated as vertical RC pier elements. The slabs are modelled as simple bilinear beam elements with concentrated plasticity at their ends. The effective length of these coupling beam elements was assumed as $l_{cb,eff} = l_{cb}$, with l_{cb} being the free span between both piers. The depth of the slab was small in comparison to the length so that the second term of Equation 1 was neglected. In order to investigate the influence of the moment introduced in the piers through the coupling beams, the effective width $b_{cb,eff}$ of the coupling beams was varied from $b_{cb,eff} = t_{URM}$ to $b_{cb,eff} = 3.0t_{URM}$, with t_{URM} representing the thickness of the URM piers. The plastic moment of the nonlinear beam varied accordingly from 4.1 kNm to 12.2 kNm. Figure 2 shows the moment profiles obtained from the pushover analysis at the peak strength of the structure. The tests presented in the following simulated internal piers. The results of the pushover analyses with different effective beam widths showed that the height of zero moment H_0 of internal piers varied approximately between $0.5H$ and $1.5H$.

DETERMINATION OF BOUNDARY CONDITIONS FOR QUASI-STATIC CYCLIC TESTS ON MASONRY PIERS

The piers were tested in the test stand shown in Figures 3 and 4. The test stand allowed applying two vertical forces and one horizontal force. The three actuators were controlled in a fully coupled mode. All piers were 2.01 m long, 2.25 m high and 0.20 m thick. For the construction of the masonry piers a typical modern Swiss hollow clay brick and a commercial cement mortar

mixture was used. The dimensions of the bricks are 190 x 300 x 195 mm (HxLxW, Figure 5). The head and bed join t thicknesses were 10-12 mm and all jo ints were fully mortared. The average compression strength of the bricks was 35 MPa and the average compression strength of the mortar was 10.5 MPa. In the first phase of the project, the boundary conditions of an internal wall at ground level were sim ulated (see Figure 1.a). In a second phase, also an external wall with varying normal force will be investigated. The following boundary conditions were defined for the three test units PUP1-3 of the first phase of the project:
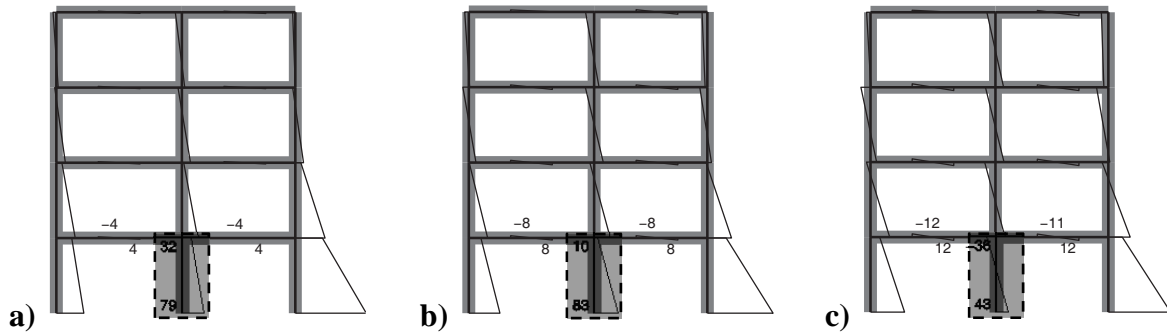
Figure 2: Results from Tremuri computations, moment diagram for an assumed effective beam width of (a) $b_{cb,eff} = t_{URM}$, (b) $b_{cb,eff} = 2.0t_{URM}$ and (c) $b_{cb,eff} = 3.0t_{URM}$.

• Constant normal force
Assuming symmetrical coupling from both sides of the internal pie r, the normal force will not change when the wall is subjected to late ral loading. Hence, the normal force is independent from the degree of coupling. To all three test units PUP1-3 the same constant normal force was applied. It was determ ined from the reference structure and corresponded to the n ormal force level due to gravity loads only. The norm al force applied to one pier was 419 kN. Thi s corresponds to a norm al stress ratio of $\sigma_0/f_u = 0.18$, where f_u represents the average compression strength of th e investigated masonry ($f_u = 5.85$ MPa) and σ_0 the average applied normal stress.

• Reference test unit PUP1
For the first test unit PUP1 standard fixed-fixed boundary conditions were applied, i. e. the rotation of the top beam was controlled to be zero. The corresponding control functions for the two vertical pistons are summarized in Table 1.

• Reduced rotational top constraints for PUP2 and PUP3
Figure 2 shows that the fixed-fixed boundary conditions are not rep resentative for the m oment profiles over the height of an internal pier of the first storey. The bottom moment is larger than the top moment and for weak coupling the top and bottom moment might even have the sam e sign. Thus, test units P UP2 and PUP3 were allo wed a lim ited rotation at the to p of the pier. Instead of imposing a certain rotation at the top, the height of zero moment H_0 was kept constant throughout the test, i.e. moment applied at the top was a function of the applied horizontal force. Therefore, the forces applied by the two vertical actuators were a function of the horizontal force and the total normal force which was kept constant throughout the test. F or PUP2 and PUP3, the

zero moment height was kept constant at $H_0 = 0.75H$ and $H_0 = 1.5H$, respectively (Figure 3). The corresponding control functions for the two vertical actuators are summarized in Table 1.
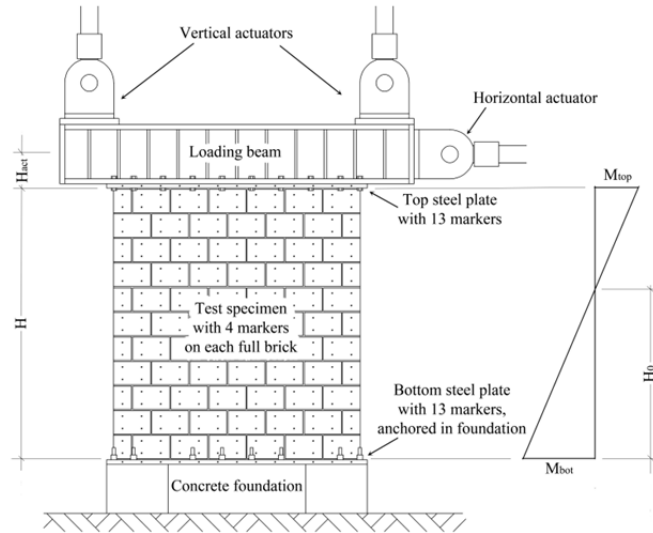

Figure 3: Test setup with layout of LEDs for optical measurements.

Table 1: Boundary conditions for PUP1-3.

Specimen	Normal stress ratio	Degree of coupling	Zero moment height H_0	Control functions for the vertical actuators
PUP1	0.18	High	$0.5H$	Actuator 1 – Force-controlled: $$F_{ver,1} = N - F_{ver,2}$$ Actuator 2 - Disp.-controlled: $$U_{ver,2} = U_{ver,1}$$
PUP2	0.18	High to intermediate	$0.75H$	Act. 1 & 2 – Force-controlled: $$F_{ver,1,2} = \frac{N}{2} \pm const \cdot F_{hor}$$
PUP3	0.18	Intermediate	$1.5H$	

|	
H	Height of the pier
H_0	Height of the zero moment
N	Normal force applied to the pier
$F_{ver,1,2}$	Forces in the two vertical actuators
F_{hor}	Force in the horizontal actuator
$U_{ver,1,2}$	Vertical displacement of the two vertical actuators with respect to the foundation
$const.$	Constant describing the dependency between $F_{ver,1,2}$ and F_{hor} which determines the moment profile. The value of this constant is different for PUP2 and PUP3.
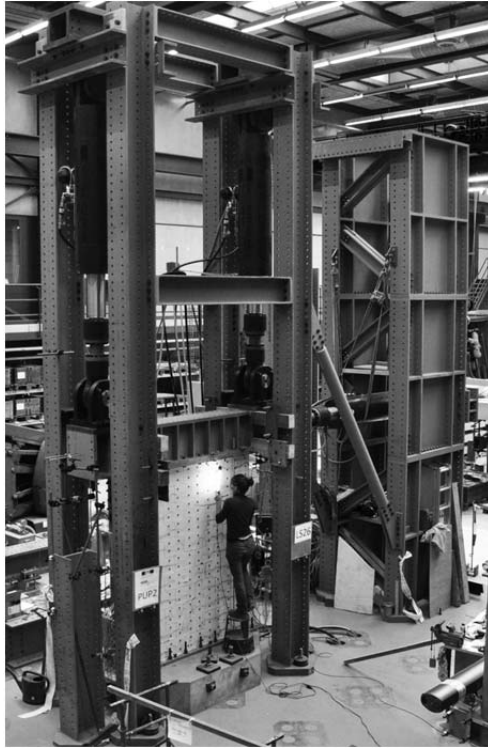
Figure 4: Photo showing the test setup for the quasi-static cyclic tests on the piers.

QUASI-STATIC CYCLIC TESTS ON MASONRY PIERS

All three tests were perf ormed applying the foll owing procedure: (0) Zero m easurements were taken before any of the three ac tuators was connected to the test un it (load step LS 0). (1) The vertical actuators were fixed to the loading beam at the top of the pier. (2) The vertical force was applied by means of the two vertical actuators (LS1). The forces applied by the two actuators were equal ($F_{ver,1,2} = N/2$); the resulting vertical force acted therefore at the centre line of the pier. (3) After applying the vert ical load, the ho rizontal actuator was fixed to the loading beam. (4) Once the horizontal actuator was connected to the loading beam, the control functions for the vertical actuators were changed to the control functions indicated in T able 1. (5) The late ral loading history was started (LS2 – end). A lo ad step of the dr ift-controlled loading history corresponds to the peak of one half-cycle. At each load step, the loading was stopped, cracks were marked and photos were taken.

The amplitudes of the half-cycles corresponded to the following drift levels: 0.025%, 0.05%, 0.1%, 0.15%, 0.2%, 0.3%, 0.4%, 0.6%, 0.8%, 1.0% (Figure 6). Note th at the cycles with amplitudes of 0.15% and 0.25% were not included in the loading history applied to PUP1, but added from PUP2 onwards since the performance of PUP1 deteriorated rapidly within the cycles with amplitudes of 0.2% and 0.3%. Cycles with amplitudes limited by forces, which are often included at the beginning of a loading history, were omitted in order to simplify the comparison of different test units within this test series.
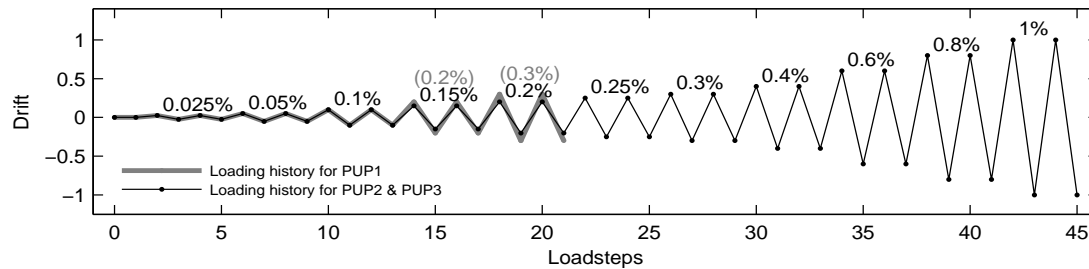
**Figure 5: Loading history of the piers.**

For all the test units, th e loading was continued until the piers were no longer able to carry th e applied vertical load. Th erefore, within this series, two different failure limit states are distinct: (1) the horizontal load failure when the strength dropped to 80% of the peak strength and (2) the vertical load failure when the pi ers can no longer sustain the vertical load applied by the vertical pistons. The definition of the hor izontal load failure corresponds to the de finition of the lim it state "Near Collapse" as defined in Eurocode 8, Part 1 [5, 6].

BEHAVIOUR OF THE PIERS DURING TESTING
The first pier, PUP1, was tested under fixed-fixed boundary conditions. Hence, the zero moment height was at approximately 0.5H (see Figure 6.c). The peak load in positive and neg ative loading direction was reached at drifts of +0.15% and -0.12%, respectivel y (see points A+/- in Figure 6.b). After the peak load was attained, th e lateral force started dropping imm ediately and horizontal load failure was reached at a drift of +0.29% and -0.17%, respectively (see points B+/- in Figure 6.b). During the cycle with a nom inal drift amplitude of 0.2%, the horizontal actuator was not stopped in time and the pier was accidentally loaded up to a drift of 0.3%. After a second full cycle of 0.2%, the pier collapsed before reaching again a drift of 0.3% (see point C in Figure 6.b).

The second pier unit, P UP2, was test ed with a zero m oment height of 0.75H (see Figure 8.c). The peak load was reached at drifts of +0.35% and -0.37%, re spectively (see points A+/- in Figure 7.b). When loading for a second time to a drift of +0.4%, the horizontal force dropped and horizontal load failure was attain ed for the positive direction of loading. Upon load reversal, the test unit did not regain 80% of its peak strength. Hence, the drift limit associated with horizontal load failure could only be reached in the positive load ing direction a nd not for t he negative loading direction (see Figure 7.b).

The third pier, PUP3, was tested with a zero m oment height of 1.5H (Figure 8.c). The peak load was attained at drifts of +0.48% and -0.75%, resp ectively. The large differences in drifts for the two directions are due to the slightly different shape of the plateaus. If the envelope is approximated by a bilinear curve, the plateau starts for both directions at a drift of around ±0.5%. The end of this plateau is reach ed at a drift of +0.69% and -0.75%, respectiv ely. At a drift of +0.69% in the positive directi on, the lateral resistance droppe d suddenly to 67%, whic h corresponds to horizontal load failure. In the nega tive direction, the pier c ould resist the lateral load until a drift of -1.0% when the force dropped to 78%.
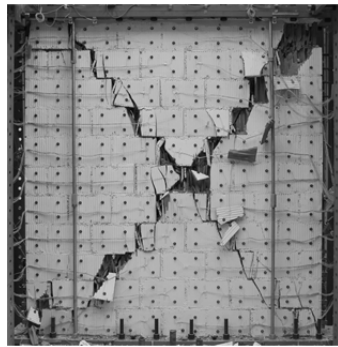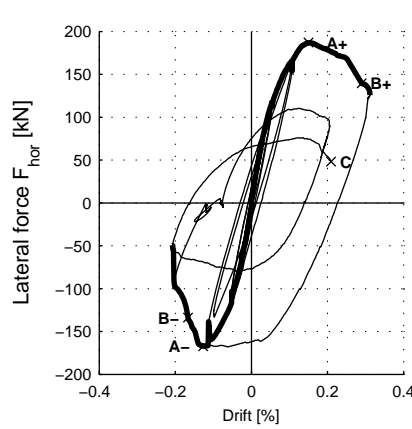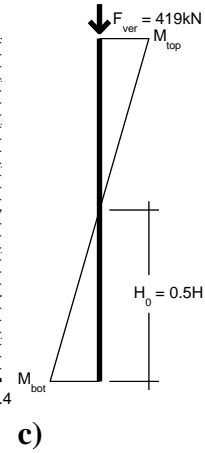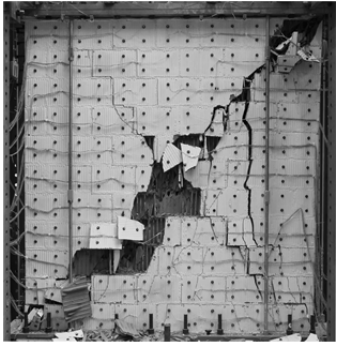
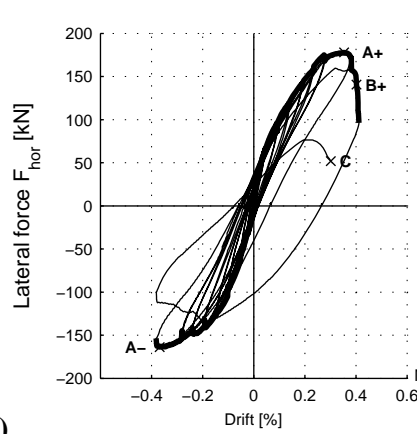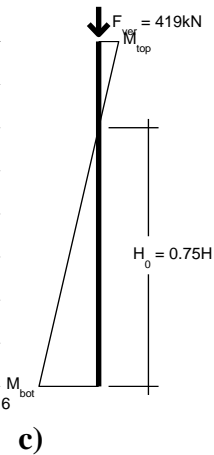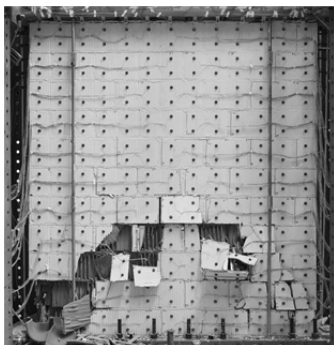**Figure 6: PUP1 (a) Photo after axial load failure, (b) displacement-force hysteresis and (c) moment diagram.**

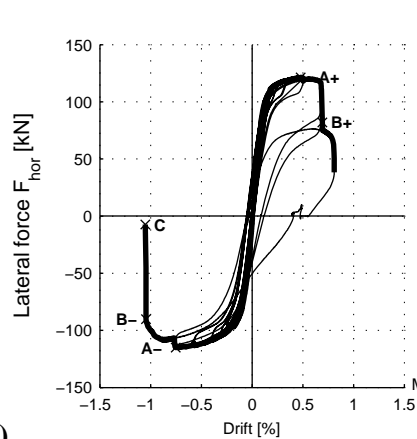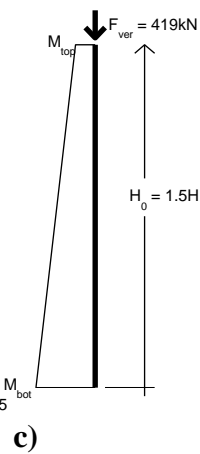**Figure 7: PUP2 (a) Photo after axial load failure, (b) displacement-force hysteresis and (c) moment diagram.**

Figure 8: PUP3 (a) Photo after axial load failure, (b) displacement-force hysteresis and (c) moment diagram.

COMPARISON OF TEST RESULTS WITH EUROCODE 8 PART 3

In Eurocode 8, Part 3, the drift capacity of m asonry piers is given as a function of the failure mode [5]. Hence, before estimating the drift capacity of a pier, its failure mode needs to be determined. The flexural and shear capacity are given by Equations 3 and 4, respectively. The smaller value of the two determines the failure mode.

$$V_f = \frac{LN}{2H_0}(1 - 1.15\,\vartheta_d) \tag{3}$$

$$V_f = f_{vd}L't \tag{4}$$

where L is the length of the pier, L' the length of the compression zone, N the normal force and H_0 the zero moment height. The parameter ϑ_d accounts for the normal stress ratio and is defined as:

$$\vartheta_d = \frac{N}{Ltf_d} \tag{5}$$

with f_d being the compression design strength of the masonry. The shear design strength f_{vd} can be computed as:

$$f_{vd} = f_{vd0} + 0.4\frac{N}{L't} \leq 0.065 f_{mk} \tag{6}$$

Once the failure m ode is determined, the drift capacity corresponding to the lim it state "Near Collapse" can be estim ated as $\frac{4}{3} \cdot 0.4\% = 0.53\%$ for sh ear failure and $\frac{4}{3} \cdot 0.8\% \cdot H_0/L = 1.07\,H_0/L$ for flexural failure [5].

For a s imple comparison of the tes t results with the recom mendations of EC8, Part 3 [5], we assume a partial safety factor of unity for the material strength ($\gamma_m = 1.0$) and the characteristic compression strength is set equa l to the m ean compression strength $f_d = f_u = 5.87$ MPa that was obtained from compression tests on m asonry wallettes. From a series of shear triplet tests, we obtained a peak coh esion $f_{vd0} = 0.27$ MPa. To remove any unwarra nted conservatism, we neglect the upper limit of $0.065 f_{mk}$ in Equation 6. The length of the com pression zone L' can be computed considering a rectangular stress block with $f_c = 0.85 f_u$ (e.g. [1]):

$$N = 0.85 f_u \cdot L't \tag{7}$$

Hence, Equation 4 can be simplified as follows:

$$V_f = f_{vko} \cdot L't + 0.4N = N \cdot \frac{f_{vko}}{0.85 f_u} + 0.4N \tag{8}$$

In Figure 9.a the predicte d lateral pier strengths corresponding to shear a nd flexural failure are plotted as a function of the normal stress ratio. As the flexural strength is a function of the height of zero moment H_0 and since H_0 differed for the three test units PUP1 to PUP3, three f lexural capacity curves are plo tted. The sh ear strength is independent of the he ight of zero m oment

H_0 and therefore only one shear capacity curve is   plotted. For PUP1 and PUP2, the predicted shear strength is less th an the pred icted flexural strength. One would therefore expect a shear failure, which corresponds to the observed failure modes. For PUP3, for which the height of zero moment was largest, a flexural behaviour is predicted, which co rresponds again to the observed failure mode. For all th ree test un its, whether th ey developed a shear or flexural behaviour, the peak strength values are well predicted by the strength equations in EC8, Part 3 [5].

In Figure 9.b the predicted drift capac ity is plotted as a function of H_0/H for a constant norm al stress ratio of $\vartheta_d = 0.18$. The drift capacity increases abruptly, where the predicted failure mode changes from shear to flexure according to E quations 3 and 4. Com paring the predictions with the experimental results, the following can be   noticed: Even though a clear shear failure was observed in the first two specimens, PUP1 and PUP2, the displacement capacity increased with increasing H_0/H ratio. The d rift capacity indicated in EC8, Part 3 [5] overestim ates the drift capacity in particular for PUP1, which wa s tested under fixed-fixed boundary conditions. According to EC8, Part 3 [5], a significant in   crease in th e displacement capacity should be obtained once the failure mode changes from shear to flexure. When we consider the linear trend indicated through the dotted line in Figure 10.b, we   notice, however, that the increase in drift capacity seems to be rather independent of the failure mode.
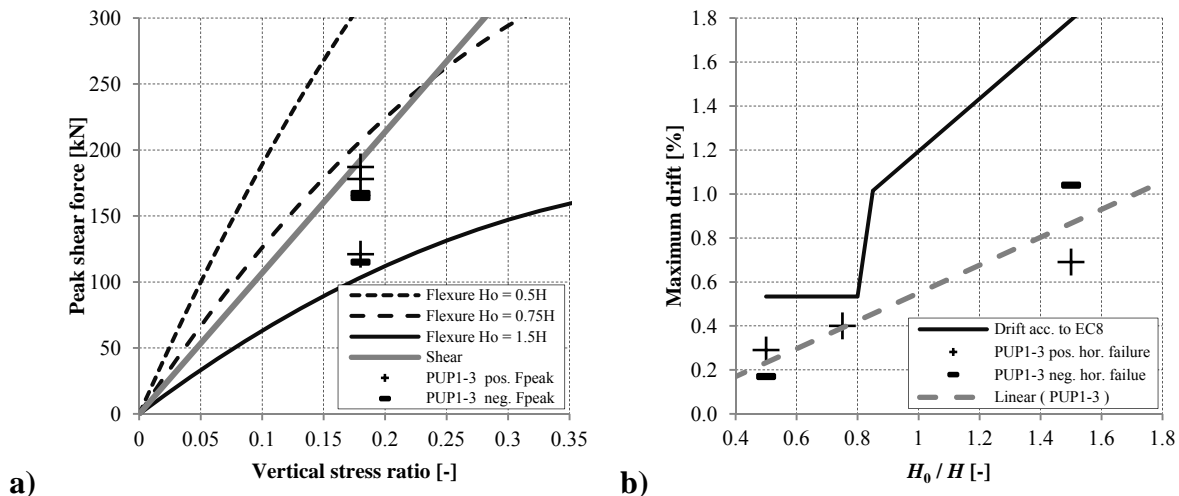

Figure 9: Comparison of the results in PUP1 to PUP3 with the recommendations from EC8, (a) prediction of the lateral force capacity and failure mode and (b) prediction of the drift capacity for the limit state "Near Collapse" [5] with the linear trend line obtained from the results for the horizontal load failure.

CONCLUSIONS AND OUTLOOK

This article presents p reliminary results of an experim   ental campaign that inv estigates the influence of coupling on the deform ation capacity of the URM piers. Pushover analysis of a reference building was carried out, where the in   fluence of the stiffness and strength on the moment profile in the f irst storey piers was illu strated. Therefore, the he ight of zero mom ent in these piers was introduced as an indicator for the degree of coupling. Accordingly, three identical piers were tested applying the sam   e normal stress while changing the zero m   oment height. Preliminary results of these tes ts are presente d and com pared with recommendations given in

EC8, Part 3 [5]. EC8 pr edicts the force capacities for all th ree piers rather well. However, the drift capacities are generally overestim ated by EC8. Furthermore, a clea r trend can be observed towards a direct dependency between the displacement capacity of the piers and the zero moment height, which seemed to be independent of the fa ilure mode. This trend is not captured by EC8, Part 3 [5].

For PUP1 to PUP3, an internal pier was the reference p ier. In internal piers th e normal force remains approximately constant when the wall is subjected to lateral lo ading. In a second phase of the project, piers were test ed under boundary conditions repres entative for outer piers where the normal force increases and decreases when the wall is subjected to cyclic lateral loading. These results will be presented e lsewhere. Furthermore, a serie s performed on half-scale pier s will allow to valid ate further the relationship between displacement capacity and z ero moment height. Additionally, models f or predicting the strength-deformation relationships of spandrel elements, which were already tes ted experimentally [7], are developed in order to allow engineers to estimate the degree of coupling and therefore the height of zero moment in the piers.

ACKNOWLEDGEMENTS

REFERENCES

[1] M. J. N. Priestley, G. M. Calvi and M. J. Kowalsky, Displacement-Based Seismic Design of Structures, Pavia: IUSS Press, 2007.

[2] S. Lagomarsino, A. Penna, A. Galasco and S. Cattari,   *Seismic Analysis Program for 3D Masonry Buildings - TREMURI user guide,* 2009.

[3] L. Gambarotta and S. Lagom arsino, "Damage models for the seism ic response of brick masonry shear walls, Part   II: the continuum   model and its applications,"   *Earthquake engineering and Structural Dynamics,* no. 26, p. 441–462, 1997.

[4] L. Gambarotta and S. Lagom arsino, "On th e dynamic response of m asonry panels," in *Proceedings of the National Conference "La meccanica delle murature tra teoria e progetto",* Messina, 1996.

[5] CEN, *Eurocode 8: Design of structures for earthquake resistance - Part 3: Strengthening and repair of buildings EN 1998-3:2004,* Brussels: European Comittee for Standardization, 2004.

[6] S. Frumento, G. Magenes, P. Morandi and G. M. Calvi, Interpretation of experim ental shear tests on clay brick masonry walls and evaluation of q-factors for seismic design, Pavia: IUSS Press, 2009.

[7] K. Beyer and A. Dazio, "Quasi-static m onotonic and cyclic tests on composite spandrels," *accepted in Earthquake Spectra,* vol. 28, no. 3, pp. 885-906, 2012.